Frontiers in Bioscience Landmark

Front. Biosci. (Landmark Ed) **2022**; 27(8): 238
https://doi.org/10.31083/j.fbl2708238

Original Research

Endostar Synergizes with Radiotherapy to Inhibit Angiogenesis of Cervical Cancer in a Subcutaneous Xenograft Mouse Model

Zhonghua Xu[1,2], Xianying Zhao[1,2], Hang Shu[1], Weiwei Luo[1], Yaqing Dong[1], Lei Xu[1], Haochen Zhu[1], Qihong Zhao[3,*], Yin Lv[1,*]

[1]Department of Radiotherapy, The First Affiliated Hospital of Anhui Medical University, 230022 Hefei, Anhui, China
[2]The Center for Scientific Research, The First Affiliated Hospital of Anhui Medical University, 230022 Hefei, Anhui, China
[3]Department of Nutrition and Food Hygiene, School of Public Health, Anhui Medical University, 230032 Hefei, Anhui, China
*Correspondence: qihong@ahmu.edu.cn (Qihong Zhao); Lvyin406@163.com (Yin Lv)
Academic Editor: Agnieszka Paradowska-Gorycka
Submitted: 10 May 2022 Revised: 9 June 2022 Accepted: 18 July 2022 Published: 10 August 2022

Abstract

Background: To investigate the synergic effect and underlying mechanism of Endostar, a recombinant human endostatin used for anti-angiogenesis, in radiotherapy for cervical cancer. **Methods**: The Cell Counting Kit-8 (CCK-8) assay and plate cloning experiment were first employed to analyze the proliferation of HeLa and SiHa cervical cancer cells and human umbilical vein vascular endothelial cells (HUVECs). Flow cytometry was used to detect apoptosis and cell cycle progression. A tube formation assay was used to assess angiogenesis *in vitro*. The expression of gamma H2A histone family member X (γ-H2AX) and activation of the vascular endothelial growth factor receptor (VEGFR) signaling pathway were detected by immunofluorescence and western blotting, respectively. In a HeLa xenograft model, tumor tissue expression of CD31 and alpha smooth muscle actin and serum expression of VEGF-A were detected by immunohistochemistry (IHC) and enzyme-linked immunosorbent assay, respectively. **Results**: The CCK-8 and plate cloning assays showed that Endostar and radiotherapy synergistically inhibited the growth of HUVECs but not HeLa and SiHa cells. The flow cytometric results showed that Endostar only promoted radiotherapy-induced apoptosis and G2/M phase arrest in HUVECs ($p < 0.05$). Endostar combined with radiotherapy also significantly inhibited tube formation by HUVECs ($p < 0.05$). Furthermore, Endostar inhibited the radiotherapy-induced expression of γH2AX ($p < 0.05$) and phosphorylation of VEGFR2/PI3K/AKT/DNA-PK in HUVECs ($p < 0.05$). IHC showed that Endostar enhanced the inhibitory effect of radiotherapy on the microvessel density in xenograft tumor tissues ($p < 0.05$), as well as serum VEGF-A expression ($p < 0.05$). The tumor volume in the combination therapy groups (1200 mm^3) was significantly lower than in the control group (2500 mm^3; $p < 0.05$). **Conclusions**: Our findings provide experimental evidence and a theoretical basis for the application of Endostar in combination with irradiation for anti-cervical cancer treatment.

Keywords: recombinant human endostatin; endothelial cell; cervical cancer; radiotherapy

1. Introduction

As the leading cause of death from gynecological tumors worldwide [1], cervical cancer has been found to be strongly associated with persistent infection with high-risk human papillomavirus (HR-HPV) [2]. Although increased awareness and use of HPV screening and vaccination has helped to reduce the incidence and mortality of cervical cancer, the current 5-year survival rate for cervical cancer is only about 60% [3]. At present, surgery is the primary treatment option for patients with stage I–IIa cervical cancer, and radiotherapy can be used as a preoperative neoadjuvant treatment to reduce tumor volume prior to surgery, as well as a postoperative adjuvant treatment to eliminate residual tumor cells. However, because the efficacy of single agents still seems restricted, combination radiotherapies involving different groups of substances have been explored.

The hypervascular nature of the tumor tissue is one of the fundamental causes of high recurrence and metastasis of cervical cancer. As a highly active vascular endothelial growth factor, endostatin has been shown to inhibit the growth of a variety of solid tumors in preclinical studies [4–6], but its insolubility, instability, short half-life, and high synthetic cost severely limit its clinical application. Endostatin is a C-terminal fragment of a XVIII molecule with a molecular weight of 20 kDa and the most effective endogenous angiogenesis inhibitor currently available. Endostar was developed by Chinese scientists applying Professor Folkman's research to improve the solubility and stability of recombinant human endostatin. Xu *et al.* [7] reported that Endostar inhibits angiogenesis by downregulating the Wnt/β-catenin signaling pathway. Ling *et al.* [8] found that Endostar suppresses the VEGF-induced tyrosine phosphorylation of KDR/Flk-1 (VEGFR-2) as well as the overall VEGFR-2 expression and the activation of ERK, p38 MAPK, and AKT in HUVECs.

Additionally, the combination of anti-angiogenesis treatment with radiotherapy has found a broad range of clinical applications for cervical cancer treatment. Ke *et al.* [9] discovered that when combined with radiotherapy and chemotherapy, recombinant human endothelin can im-

Copyright: © 2022 The Author(s). Published by IMR Press.
This is an open access article under the CC BY 4.0 license.

Publisher's Note: IMR Press stays neutral with regard to jurisdictional claims in published maps and institutional affiliations.

prove the short-term efficacy of advanced cervical cancer without causing serious adverse effects. In addition, Jia *et al*. [10] found that the most significant inhibition of HeLa tumor growth and lymph node metastasis was observed with Endostar plus concurrent chemoradiotherapy (CCRT) compared with CCRT only, Endostar only, or a control group. Endostar was also found to inhibit the expression of vascular endothelial growth factor (VEGF) and hypoxia-inducible factor 1 alpha (HIF-1α) *in vivo* and *in vitro* [10]. In another recently published phase II study [11], the objective response rate and disease control rate with intensity-modulated radiation therapy (IMRT)-based CCRT plus Endostar infusions were 67.74% and 83.87%, respectively, supporting the application of this treatment for patients with pelvic locoregional recurrence of cervical cancer following surgical treatment. However, the precise cellular and molecular biological mechanisms underlying these combination therapies remain unknown.

Conversely, radiotherapy has been shown in studies to stimulate tumor angiogenesis, resulting in increased malignancy of tumor cells, which in turn promotes tumor metastasis and recurrence [12]. Tumor cells secrete a variety of cytokines in response to radiation stimulation, including VEGF and transforming growth factor β (TGF-β). Among them, VEGF can stimulate the growth of blood vessels in tumor tissues, increasing oxygen and nutrient delivery to the tumor and thus promoting its proliferation and metastasis. Pueyo *et al*. [13] subcutaneously injected irradiated A431 cells into nude mice and discovered that tumors formed by irradiated cells had a faster growth rate and more abundant angiogenesis, compared to untreated cells. Additionally, they confirmed that this aggressive phenotype is associated with the activation of radiation-induced extracellular signal-related kinases ERK1/2 (extracellular regulated protein kinase1/2, ERK1/2) and protein kinase B (PKB or Akt), as well as increased transcription of epidermal growth factor receptor (EGFR), TGF-α and VEGF. It is reasonable to speculate that anti-angiogenesis therapy administered concurrently with radiotherapy may inhibit radiation-induced angiogenesis [14].

In the present study, through cell proliferation and plate cloning experiments, we investigated the inhibitory effects of Endostar and radiotherapy on HeLa and SiHa cervical cancer cells as well as human umbilical vein endothelial cells (HUVECs). Additionally, flow cytometry and immunofluorescence were used to assess the effect of Endostar and radiotherapy on apoptosis, cell cycle distribution, and H2A histone family member X (H2AX) expression. Finally, we investigated the synergistic effect of Endostar with radiotherapy using a cervical cancer transplanted tumor model in nude mice. Our findings provide experimental evidence and a theoretical basis for the application of Endostar in anti-cervical cancer treatment in the future.

2. Materials and Methods

2.1 Cell Lines

Human cervical cancer cell lines HeLa (http://www.mjswkj.cn/atcc-list.asp?id=253&lx=small&anid=2&nid=12) and SiHa (http://www.mjswkj.cn/atcc-list.asp?id=2604&lx=small&anid=2&nid=12) were obtained from the Cell Bank of Type Culture Collection of Chinese Academy of Sciences (Shanghai, China). HUVECs (http://www.mjswkj.cn/atcc-list.asp?id=2876&lx=small&anid=2&nid=12) were purchased from MINGJING Biology. Co. Ltd. (Shanghai, China). All cells were cultured in appropriate conditions according to the suppliers' instructions.

2.2 Cell Proliferation Assay

Recombinant human endostatin, Endostar, was provided by Simcere Pharmaceutical Co., Ltd. (Nanjing, China). For *in vitro* assays, experimental groups were set up as follows: control group, radiotherapy (RT) group, Endostar (E) group, and E+RT group. Cell proliferation rates were determined by Cell Counting Kit-8 (CCK8) assay (Beyotime Biotechnology, Shanghai, China) following the manufacturer's instructions, and six replicates were tested for each group. Specifically, cells at a density of 4×10^4/mL (4000 cells/well) were seeded into 96-well plates for 16 hours followed by serum starvation overnight. In the treatment groups, the medium was replaced with complete medium containing Endostar of different concentrations and incubated for 1 hour before exposure to 12 Gy of X-ray irradiation for 24, 48 or 72 hours, without medium exchange. After the addition of 10 μL CCK-8 reagent to each well and incubation for 2 hours, the absorbance at 450 nm indicated the cell count in each sample.

2.3 Clonality Assay

After HeLa and SiHa cells had adhered to six-well plates at the density of about 500 cells/well, culture medium containing Endostar was added for incubation for 1 hour, and then X-ray irradiation of 0, 2, 4, 6, or 8 Gy was administered once, followed by a 13-day incubation period with medium exchanged every 5 days. When cell colonies were visible under the microscope, they were fixed in 4% paraformaldehyde for 20 minutes and stained with crystal violet for 15 minutes for counting the cell colonies (>50 cells were counted as one colony). The adherence and cell survival rates were calculated as follows: adherence rate = (number of colonies in the control group/number of inoculated cells in the control group) $\times$ 100%; and cell survival rate = [number of colonies/(number of inoculated cells $\times$ adherence rate)] $\times$ 100%. The survival fraction (SF) [$SF = 1-(1-e^{-D/D0})^N$] was calculated using the multi-target single-click model in GraphPad prism 8.0 (GraphPad Software Inc., CA, USA). The sensitization enhancement ratio (SER) was calculated by comparing the D0 and Dq values for each group of cells before and after treatment. All experiments were performed in triplicate.

IMR Press

2.4 Flow Cytometry for Cell Cycle and Apoptosis Assessments

A six-well plate was seeded with a well-growing single-cell suspension to achieve the optimal cell density. After the cells reached 80% confluency, Endostar and/or 12 Gy X-ray was administered for 24 hours. Cells were harvested and stained with propidium iodide (PI) after pretreatment with RNase A for cell cycle analysis. The AnnexinAbflourTM647 Apoptosis Detection Kit (Abbkine Scientific, Beijing, China) was used for cell apoptosis detection according to the manufacturer's instructions. The FACS Canto II instrument (BD Biosciences, San Diego, CA, USA) was used to perform cytometry experiments, and the software FlowJo (Version 10.0.7) (Ashland, OR) was used to analyze cell cycle and apoptosis.

2.5 In vitro Endothelial Cell Tube Formation Assay

After addition of about 75 μL/well of liquid Matrigel (Corning Inc., Corning, NY, USA) to pre-cooled 96-well plates with a pre-cooled pipette tip, the plates were placed on ice for 5 min to ensure the Matrigel was evenly distributed across each well. The plates were then incubated at 37 °C for 60 minutes to allow the gel to solidify. HUVECs were inoculated in the above 96-well plates at a density of 2 $\times$ 10^5/mL. Cells were then treated with Endostar for 1 hour, followed by 12 Gy X-ray irradiation for 3, 6 or 9 hours. The formation of endothelial tubes at each time point was observed in five randomly selected fields and photographed under an inverted microscope (magnification, 200$\times$). The formed tube area in each field was analyzed by ImageJ software (NIH, Bethesda, MD, USA).

2.6 Immunofluorescence Assay (IFA) and Western Blotting

Briefly, after fixation with 4% paraformaldehyde and permeabilization with 0.1–0.5% triton X-100, cells were incubated with primary antibody against γH_2AX (cat. no. 9718S, Cell Signaling Technology, USA) (1:400) and fluorochrome-conjugated secondary antibody (ZSGB-BIO, China) (1:1000). For western blotting, denatured total protein of cell lysate in each group were separated by sodium dodecyl sulfate (SDS)-polyacrylamide gel electrophoresis (PAGE), transferred to a polyvinylidene difluoride (PVDF) membrane and probed with primary antibodies and horseradish peroxidase (HRP)-conjugated secondary antibodies. The primary antibodies we used included anti-HIF-1α (AF1009, Affinity, USA), anti-VEGFR-2 (Sc-393163, Santa Cruz Biotechnology, USA), anti-p-VEGFR-2 (AF3279, Affinity, USA), anti-PI3K (Sc-1637, Santa Cruz Biotechnology, USA), anti-p-PI3K (AF3241, Affinity, USA), anti-AKT (4691, Cell Signaling Technology, USA), anti-p-AKT(AF0016, Affinity, USA), anti-γH2AX (9718, Cell Signaling Technology, USA), anti-DNA-PKcs (Sc-390698, Santa Cruz Biotechnology, USA), anti-p-DNA-PKcs (AF8005, Affinity, USA), and anti-β-actin (TA-09, ZSGB-BIO, USA). AffiniPure Goat Anti-Rabbit IgG (H+L) (111-005-003, Jackson Laboratories, USA) or AffiniPure Goat Anti-Mouse IgG (H+L) (115-005-003, Jackson Laboratories, USA) was used as the secondary antibody. The bands detected by an enhanced chemiluminescence (ECL) Western blot detection kit (Pierce, Waltham, MA, USA) were visualized and semi-quantified using the Gel Image System of Tanon Fine Do X6 (Tanon Science & Technology Co., Ltd., China).

2.7 Tumor Growth and Angiogenesis Evaluation in a Mouse Xenograft Model

Four- to six-week-old female BALB/C nude mice with a bodyweight of 18–22 g were obtained from the Beijing Weitong Lihua Experimental Animal Technology Co., Ltd (Beijing, China). They were bred and housed in specific pathogen-free (SPF) conditions for this study. For each mouse, 100 μL of HeLa cell suspension at 1 $\times$ 10^7 cells/mL was subcutaneously inoculated. When the tumor volume reached 150–250 mm^3, mice bearing HeLa-xenografted tumors were randomly divided into the following four groups, with 5 mice in each group: Endostar (E) group: nude mice injected with Endostar (10 mg/kg/d) through the tail vein for 24 days; RT group: the tumor area received 8 Gy/1 F irradiation on the 12th day; E+RT group: after administration of Endostar for 1 hour, the tumor area was irradiated with 8 Gy/1F; and the control group: injection of an equal volume of normal saline. In detail, mice were intraperitoneally anesthetized with 4% chloral hydrate, then the tumor region of the E+RT group mice was irradiated with 8 Gy X-ray. Tumor volume (mm^3) was measured with a vernier caliper and estimated using the following formula: tumor volume = $1/2ab^2$, where a is the longest diameter and b is the transverse diameter in mm. The bodyweight of the nude mice and the size of the subcutaneous transplanted tumors were recorded in detail for plotting of tumor growth curves. On day 28, mice were sacrificed via cervical dislocation following anesthesia with 4% chloral hydrate. The tumors were removed, photographed and measured. The histology of transplanted tumor specimens was observed by conventional hematoxylin and eosin (H&E) staining and light microscopy. In addition, the expression levels of CD31 and alpha smooth muscle action (αSMA) were measured by immunohistochemistry (IHC), and the microvessel density and αSMA expression in the slices of each group were analyzed by the software Image Pro Plus (Media Cybernetics, MD, USA). The levels of VEGF in serum were measured by enzyme-linked immunosorbent assay (ELISA) according to the manufacturer's instruction (MEIMIAN, Jiangsu, China). All protocols were reviewed and approved by the Institutional Animal Care and Use Committee at Anhui Medical University (No. LLSC20201146).

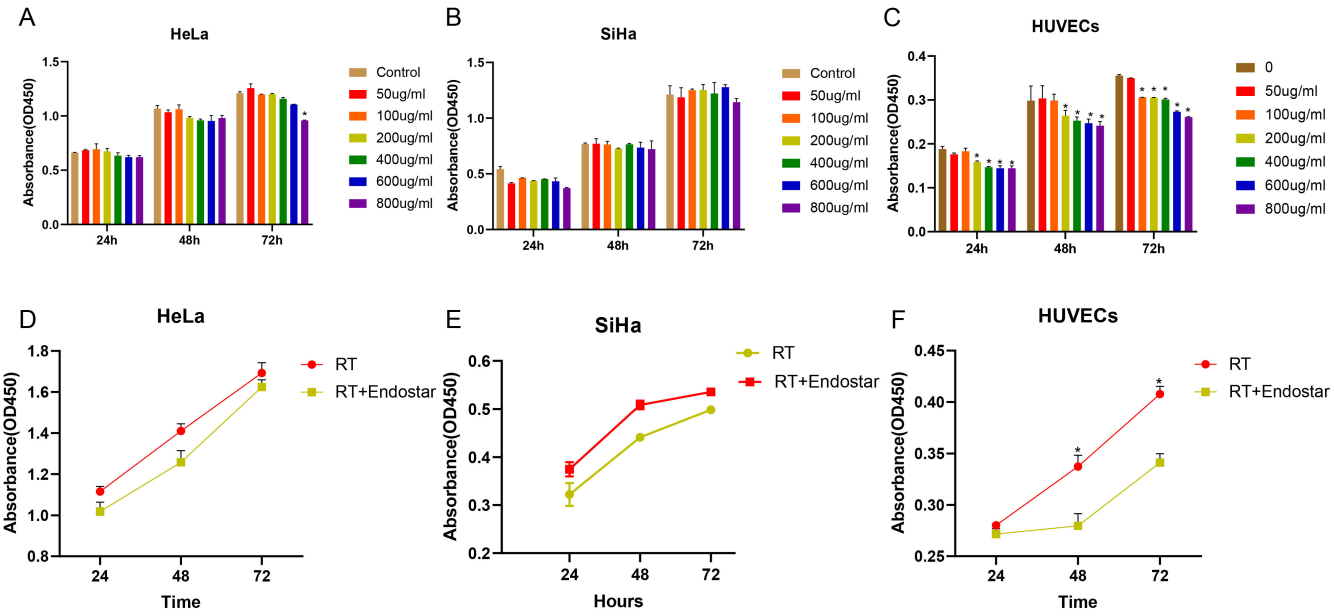

Fig. 1. Endostar and irradiation synergistically inhibited the proliferation of endothelial cells but not cervical cancer cells. HeLa cells (A), SiHa cells (B) and HUVECs (C) were treated with the different concentrations of Endostar for 24, 48, or 72 hours. HeLa cells (D), SiHa cells (F) and HUVECs (F) were further treated with 200 μg/mL Endostar in combination with 12 Gy of X-ray irradiation for 24, 48, or 72 hours. Cell viability was assessed by CCK-8 assay, and the mean $\pm$ standard deviation inhibition rate based on the OD_{450} values were obtained from independent experiments.

2.8 Statistical Analysis

All data were analyzed using SPSS 18.0 software (IBM, Armonk, NY, USA). Measured data are expressed as mean $\pm$ standard deviation. Comparisons between two groups were made by the *t*-test, and comparisons among multiple groups were made by one-way analysis of variance (ANOVA). The IHC results were analyzed by the χ^2 test. Two tailed $p < 0.05$ was considered statistically significant.

3. Results

3.1 Endostar and Radiotherapy Synergistically Inhibited the Growth of Endothelial Cells but not Cervical Cancer Cells in Vitro

The CCK-8 assay was used to determine the effect of different concentrations of Endostar on the proliferation of HeLa cells, SiHa cells, and HUVECs after treatment for 24, 48 and 72 hours. As shown in Fig. 1C, at each time point, Endostar inhibited the growth of HUVECs beginning at a concentration of 200 μg/mL, and the effect was steadily strengthened as the concentration increased ($p < 0.05$). However, for HeLa and SiHa cells, Endostar did not show a significant dose-dependent growth inhibitory effect at any time point (Fig. 1A,B). As a result, the concentration of 200 μg/mL Endostar was applied in the subsequent experiments. A number of experiments were further conducted to determine whether irradiation would enhance Endostar-mediated cell growth inhibition. As shown in Fig. 1F, the OD_{450} value for the RT+Endostar-treated HUVECs was significantly lower than that for HUVEC cells treated by RT alone beyond 48 hours post-treatment ($p < 0.05$). In contrast, the OD_{450} values did not differ significantly between HeLa or SiHa cells treated with RT+Endostar and RT only. Consistently, the results of the colony formation assay found that in HeLa or SiHa cells treated with the same RT dose, the addition of Endostar did not significantly change the cell survival score (Fig. 2A,B), indicating that Endostar had no measurable impact on the radiotherapy sensitivity of these cervical cancer cells. These results collectively indicate that Endostar can synergize with RT to inhibit HUVEC growth *in vitro*.

3.2 Endostar and Radiotherapy Synergistically Induced Apoptosis and Cell Cycle Arrest in Endothelial Cells in Vitro

Annexin-V/PI double staining was performed to assess treatment-induced apoptosis. The results indicated that compared to those of the untreated groups, the apoptosis rates of HeLa cells (Fig. 3A), SiHa cells (Fig. 3B), and HUVECs (Fig. 3C) were significantly higher in the RT group ($p < 0.05$), but were unaffected by Endostar treatment. Interestingly, the apoptosis rate of HUVECs, but not of HeLa or SiHa cells, was notably higher in the Endostar+RT group than in the RT monotherapy group ($p < 0.05$, Fig. 3). As illustrated in Fig. 4C, cell cycle detection by flow cytometry showed that, compared with that in the control group, the ratio of HUVECs in G0/G1 phase in the Endostar+RT

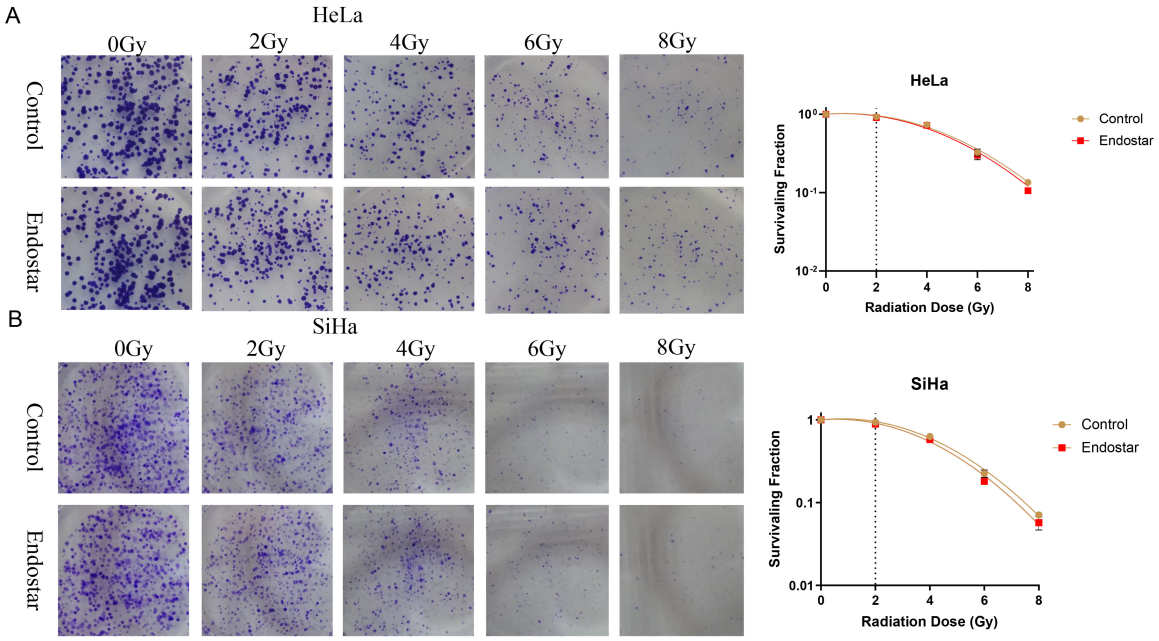

Fig. 2. The effects of Endostar and its combination with radiotherapy on the clonogenic ability of HeLa cells (A) and SiHa cells (B). In HeLa or SiHa cells treated with the same RT dose, the addition of Endostar did not significantly change the cell survival score, indicating that Endostar had no measurable impact on the radiotherapy sensitivity of cervical cancer cells.

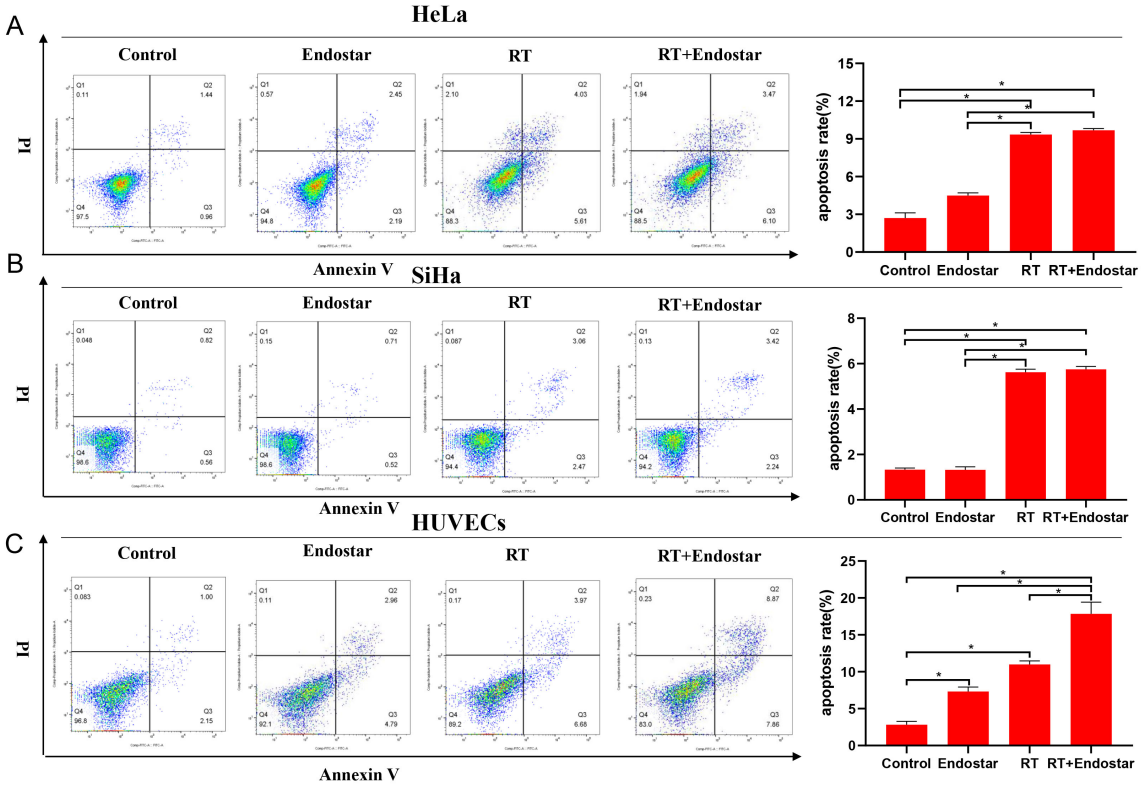

Fig. 3. Endostar and radiotherapy synergistically induced apoptosis of endothelial cells. Flow cytometry indicated that compared to those in the untreated groups, the apoptosis rates of HeLa cells (A), SiHa cells (B), and HUVECs (C) were significantly higher in the RT group ($p < 0.05$), but were unaffected by Endostar treatment. The apoptosis rate of HUVECs, but not of HeLa or SiHa cells, was notably higher in the Endostar+RT group than in the RT monotherapy group ($p < 0.05$).

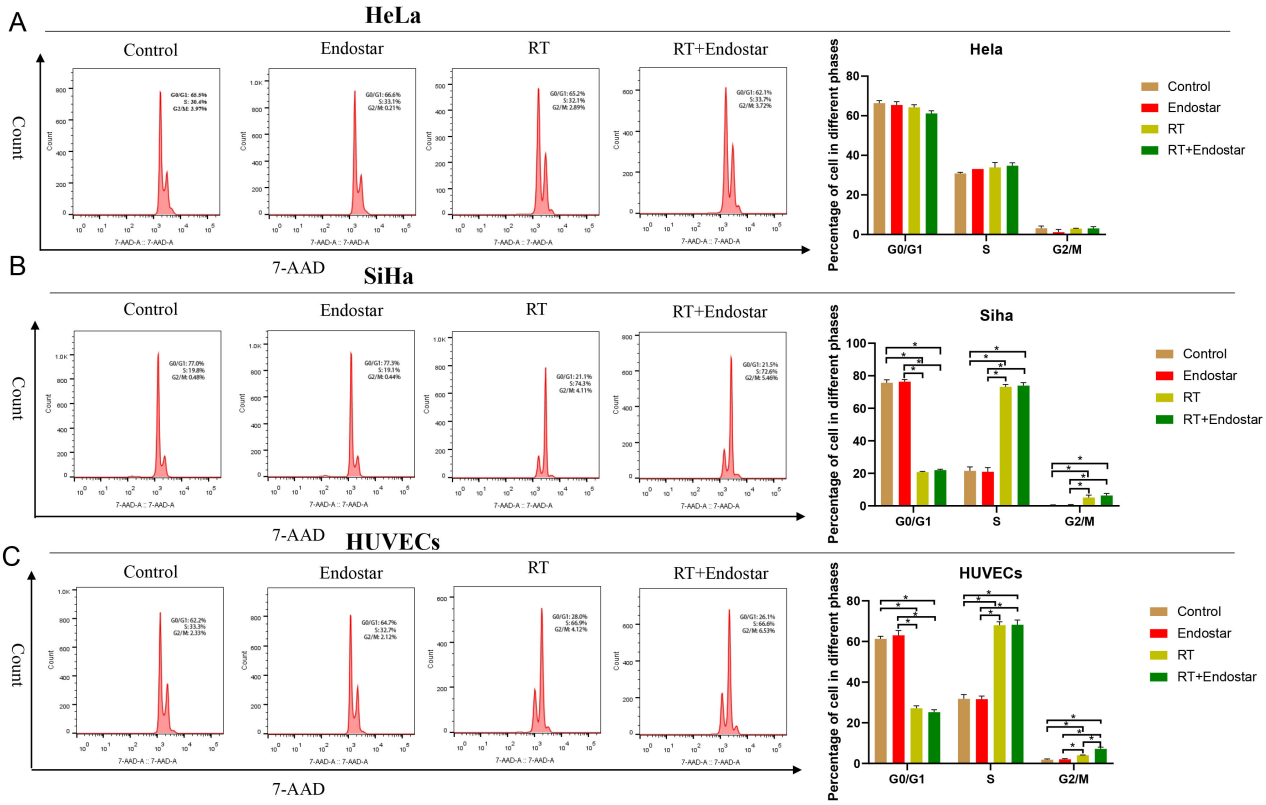

Fig. 4. Endostar and radiotherapy synergistically induced cell cycle arrest of endothelial cells. Neither the Endostar+RT group nor the RT monotherapy group showed a significant difference in the proportions of HeLa (A) or SiHa cells (B) in each cell cycle phase. (C) Compared with that in the control group, the ratio of HUVECs in G0/G1 phase in the Endostar+RT group or RT monotherapy group was significantly reduced, while the proportions of cells in S and G2/M phases were increased significantly ($p < 0.05$). Compared with that in the RT monotherapy group, the ratio of HUVECs in G2/M phase was increased ($p < 0.05$).

group or RT monotherapy group was significantly reduced, while the proportions of cells in the S and G2/M phases were increased significantly ($p < 0.05$). However, compared with that in the RT monotherapy group, the ratios of HUVECs in the G0/G1 and S phases did not differ significantly in the Endostar+RT group, while the ratio of G2/M phase cells was increased ($p < 0.05$), indicating that RT reduce the proportion of HUVECs in the G0/G1 phases and arrested them in the S and G2/M phases. Moreover, Endostar promoted a further G2/M phase arrest of HUVECs. In line with the apoptosis findings, neither the Endostar+RT group nor the RT monotherapy group showed significant differences in the proportions of HeLa (Fig. 4A) or SiHa cells (Fig. 4B) in each cell cycle phase. Due to the fact that G2/M phase cells are the most radiosensitive, our findings indicated that Endostar could increase HUVEC radiosensitivity by increasing the proportion of these cells in G2/M phase.

3.3 Endostar Combined with Radiotherapy Inhibited Tube Formation by Endothelial Cells in Vitro

Angiogenesis is characterized by the formation of capillary tubes and the sprouting of new capillaries during solid tumor growth. To evaluate the therapeutic effects of Endostar and radiotherapy on this reorganization stage during angiogenesis, an *in vitro* tube formation assay was performed. As displayed in Fig. 5, microscopic observation showed that the arrangement of the tubes in the negative control group was essentially complete after 3 hours, while that in the treatment group was incomplete and had a sparse network. The quantitative results also showed that compared with that in the control group, the capillary area was significantly inhibited in each treatment group at each time point. Additionally, the inhibition rate was noticeably higher in the Endostar+RT combination group than in the corresponding monotherapy groups ($p < 0.05$). These results demonstrate that the tube formation of HUVECs was inhibited more by the synergistic effect of Endostar and RT.

3.4 Endostar Inhibited RT-Induced DNA Damage Repair in HUVECs in Vitro

By evaluating the γH2AX (Ser139 site)-mediated repair of DNA double-strand breaks, we further explored the effect of recombinant human endostatin on the DNA damage induced by radiotherapy [15] (Fig. 6). The results showed that 1 hour after treatment, compared to that in

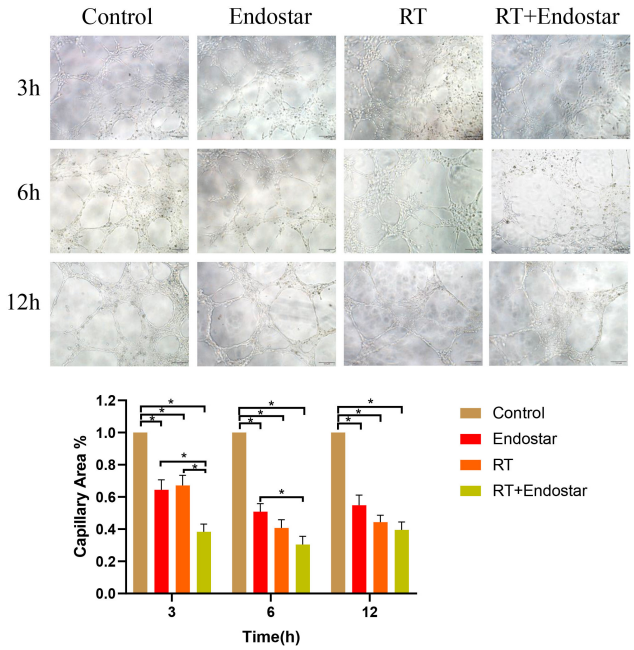

Fig. 5. Endostar combined with radiotherapy inhibited tube formation by endothelial cells *in vitro*. Microscopic observation showed that the arrangement of the tubes was incomplete and had a sparse network in the treatment group. The quantitative results also showed capillary area was significantly reduced in each treatment group at each time point. Additionally, the inhibition rate was noticeably higher in the Endostar+RT group than in each monotherapy group ($p < 0.05$).

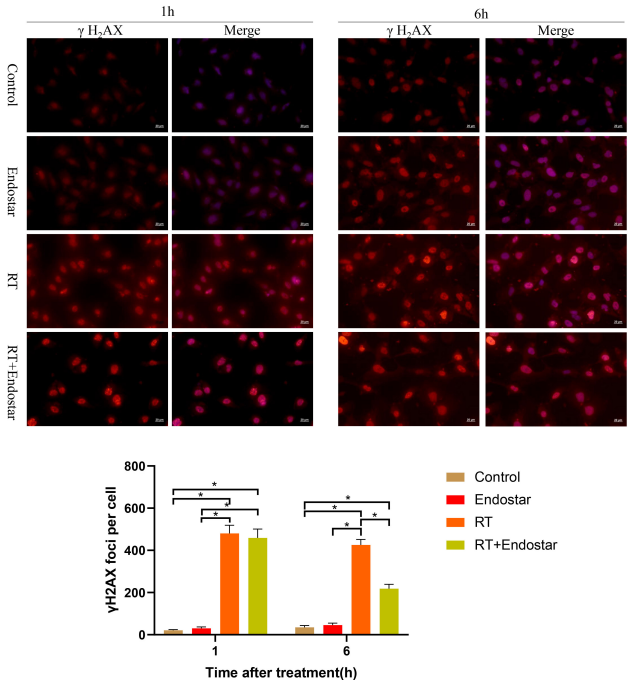

Fig. 6. Endostar inhibited RT-induced DNA damage repair in HUVECs *in vitro*. One hour after treatment, the expression of γH2AX was increased significantly ($p < 0.05$) in HUVECs of the RT group and the Endostar+RT group. After 6 hours of treatment, while H2AX expression in HUVECs remained significantly higher in the RT and Endostar+RT groups than in the control group ($p < 0.05$), it was significantly lower in the Endostar+RT group than in the RT monotherapy group ($p < 0.05$).

the control group, the expression of γH2AX in the HUVECs of the RT group and the Endostar+RT group was increased significantly ($p < 0.05$), but no significant difference was fonud between the Endostar+RT group and the RT monotherapy group. However, after 6 hours of treatment, while H2AX expression in HUVECs remained significantly higher in the RT and Endostar+RT group than in the control group ($p < 0.05$), it was significantly lower in the Endostar+RT group than in the RT monotherapy group ($p < 0.05$), suggesting that Endostar can inhibit RT-induced DNA damage repair in HUVECs *in vitro*.

3.5 Endostar Increased HUVEC Radiosensitivity via the VEGFR2/PI3K/AKT/DNA-PKcs Pathway

The above results led us to hypothesize that Endostar may enhance HUVEC radiosensitivity by inhibiting DNA repair via the VEGF receptor (VEGFR) pathway (Fig. 7). To test this hypothesis, we examined the expression regulation of VEGFR and its downstream signaling molecules in HUVECs treated with gradient concentrations of Endostar in combination with RT. Western blotting analysis revealed that, in comparison to RT monotherapy, Endostar+RT significantly inhibited the phosphorylation of VEGFR, PI3K, AKT, and DNA-PKcs in HUVECs ($p < 0.05$). Simultaneously, H2AX expression was decreased significantly ($p < 0.05$), but not according to a dose-dependent response to Endostar, consistent with the immunofluorescence staining results. These results indicate that Endostar may affect HUVEC survival following RT administration via the VEGFR2/PI3K/AKT/DNA-PKcs pathway, without affecting HIF-1 expression.

3.6 Endostar cannot Directly Inhibit Cervical Tumor Growth in Vivo

To study the effect of Endostar on the growth of subcutaneously transplanted tumors of HeLa cells, we started daily tail vein injection of Endostar when the tumor volume reached 70–150 mm^3 and started 8 Gy radiotherapy treatment 12 days later. As presented in Fig. 8A,B, there was no significant difference in the volume of transplanted tumors between each group prior to radiotherapy, indicating that Endostar had no obvious antitumor effect. The sizes of tumors in the RT monotherapy and Endostar+RT groups significantly decreased by the fourth day following radiotherapy, compared to the control group ($p < 0.05$). The tumors in the Endostar+RT group shrank slightly less than those in the RT monotherapy group, but without a statistically significant difference. Furthermore, the results for tumor weight changes, which were similar to the tumor vol-

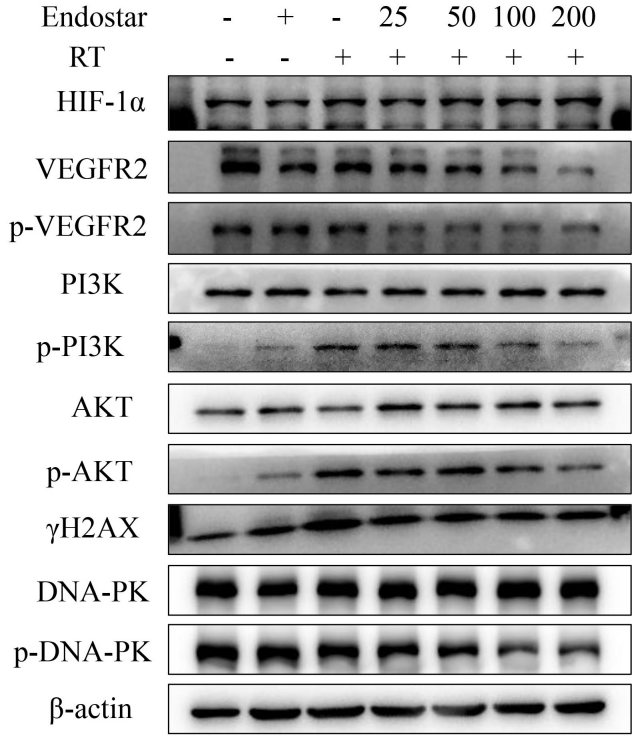

Fig. 7. The effect of Endostar on HIF-1α/VEGFR2/PI3K/AKT/DNA-PKcs pathway activation after radiotherapy in HUVECs. Western blotting analysis revealed that in comparison with RT monotherapy, Endostar+RT significantly inhibited the phosphorylation of VEGFR, PI3K, AKT, and DNA-PKcs in HUVECs ($p < 0.05$). Simultaneously, H2AX expression decreased significantly ($p < 0.05$).

ume change trend, indicated that Endostar failed to significantly promote the inhibitory effect of radiotherapy on tumor growth (Fig. 8B,C). Although mice in both RT groups lost about 10% of their body weight from day 13 to the endpoint, the body weight in the two RT groups did not differ significantly, indicating that Endostar had no noticeable effect on the animals' growth (Fig. 8D).

3.7 Anti-Angiogenic Effects of Endostar in Tumor Xenografts

The density of microvessels in xenografted tumors was quantified using immunohistochemical staining for the endothelial cell marker CD31. After treatment, the tumor microvessel density was significantly decreased in all three treatment groups compared with that in the control group ($p < 0.05$). Moreover, the tumor microvessel density was notably lower in the Endostar+RT group than in the RT monotherapy group ($p < 0.05$; Fig. 9A,B). On the other hand, although expression of αSMA, a pericyte marker, was significantly decreased in all three treatment groups ($p < 0.05$), no obvious difference was observed between the Endostar+RT and RT monotherapy groups (Fig. 9A,C), indicating that the Endostar-mediated enhancement of the inhibitory effect of radiotherapy on microvessel density was endothelial cell specific. Additionally, the results of ELISA demonstrated that in comparison with the control group, only the Endostar+RT treatment but not the corresponding monotherapy significantly reduced VEGF levels in the serum of nude mice ($p < 0.05$; Fig. 9D).

4. Discussion

Recent basic research on recombinant endostatin has revealed that it has the ability to inhibit endothelial cell migration and tubule formation, as well as to block tumor nutrient supply, thereby inhibiting tumor proliferation and metastasis [16]. Additionally, studies have demonstrated that recombinant human endostatin can induce apoptosis in tumor cells and vascular endothelial cells [17] as well as inhibit the G2/M phase transition, thereby affecting tumor radiotherapy sensitivity [18,19]. In the present study, we discovered that Endostar in gradient concentrations inhibited HUVEC proliferation without impairing HeLa or SiHa growth. Additionally, Endostar and its combination with radiotherapy inhibited HUVEC growth but had no apparent synergistic effect on cervical cancer cells. Flow cytometric results revealed that Endostar promoted apoptosis and G2/M phase arrest in HUVECs compared to control treatment, which was further enhanced by combination with radiotherapy, but had no effect on HeLa or SiHa cells. Tubule formation experiments demonstrated that both Endostar and radiotherapy treatments could inhibit tubule formation by HUVECs, and the effect was further strengthened by combination of these therapies.

Endostar has been shown in signaling pathway research to inhibit tumor angiogenesis by down-regulating the expression of VEGF and VEGFR [8]. Endostar can also inhibit other key signaling pathways, including HIF-1α, matrix metalloproteinase-2 (MMP-2), basic fibroblast growth factor (bFGF), and the integrin $\alpha v\beta 3$ pathway, thereby regulating the tumor microenvironment and promoting blood vessel normalization [20]. In this study, we found that Endostar in combination with radiotherapy decreased VEGFR, PI3K, and AKT phosphorylation expression but had no effect on HIF-1 expression in endothelial cells, suggesting that the combined treatment had no effect on the hypoxic state of cervical cancer.

Recent research has discovered a link between the inhibition of angiogenesis and DNA damage repair. Raffaella *et al.* [21] discovered that siRNA-mediated silencing of AKT decreased DNA-PKcs (Thr2609) phosphorylation, indicating that AKT regulates DNA-PKcs expression [22]. Additionally, studies have shown that when exposed to radiation, epidermal growth factor receptor (EGFR) translocates to the nucleus to regulate DNA-PKcs activity and promote double-strand break repair [23], and that VEGF influences radiation-induced changes in EGFR subcellular localization [24]. Endostatin was found to promote DNA damage in colon cancer cells by interacting with DNA-PKcs

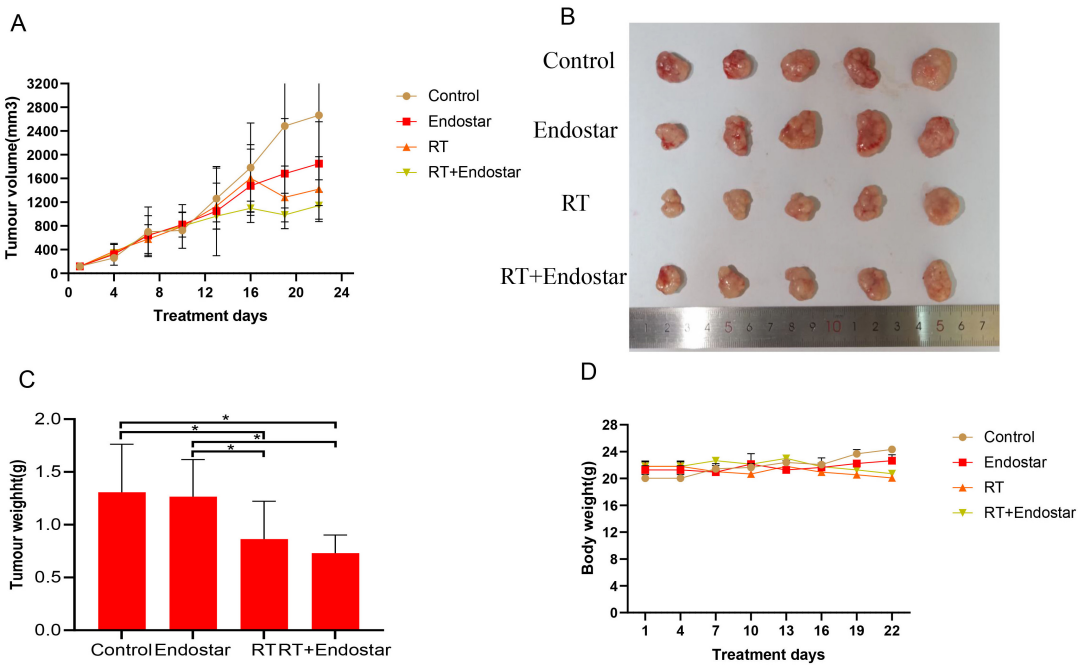

Fig. 8. Endostar cannot directly inhibit cervical tumor growth *in vivo*. (A,B) Tumor volume did not differ significantly between the groups prior to radiotherapy. Tumor size in the RT monotherapy and Endostar+RT groups was significantly decreased on the fourth day following radiotherapy ($p < 0.05$). (C) The results for tumor weight changes also indicated that Endostar failed to significantly promote the inhibitory effect of radiotherapy on tumor growth. (D) The body weight of nude mice in each group did not change significantly during the continuous treatment.

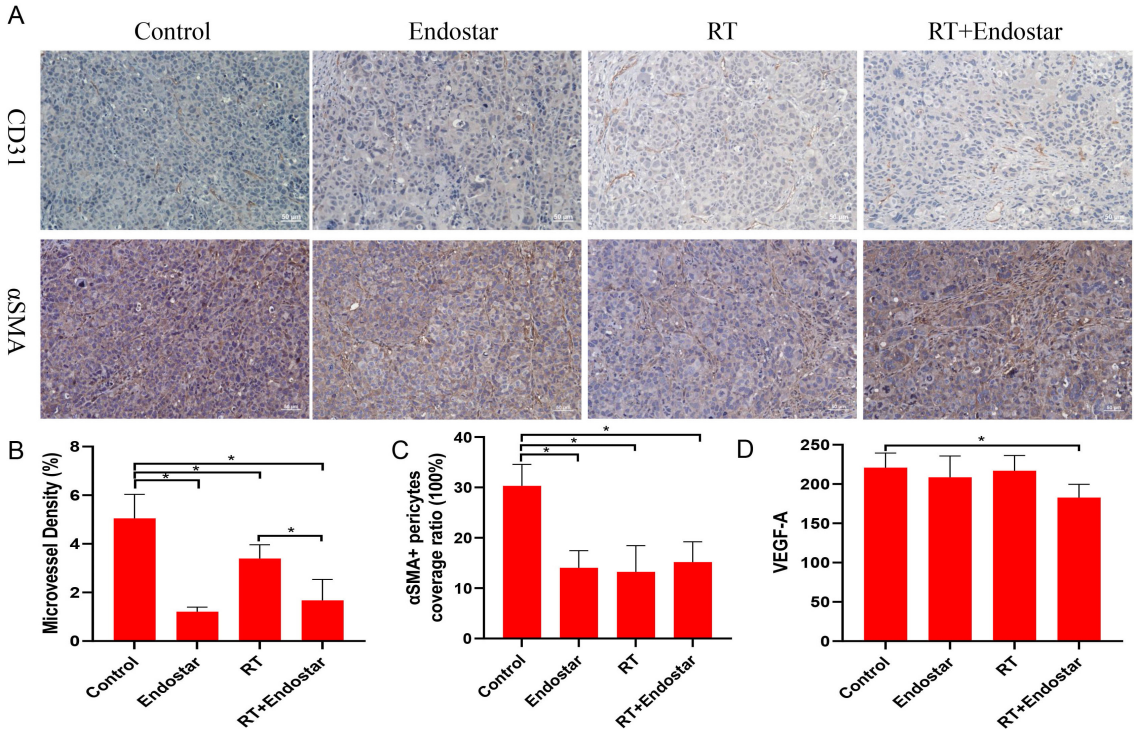

Fig. 9. Anti-angiogenic effects of Endostar and radiotherapy in tumor xenografts. (A,B) The tumor microvessel density was significantly decreased in all three treatment groups ($p < 0.05$), and was notably lower in the Endostar+RT group than in the RT monotherapy group ($p < 0.05$). (A,C) The expression of αSMA was significantly decreased in all three treatment groups ($p < 0.05$), but no obvious difference was observed between the Endostar+RT and RT monotherapy groups. (D) ELISA results indicated that only Endostar+RT but not the corresponding monotherapy significantly reduced VEGF levels in the serum of nude mice ($p < 0.05$).

[25]. Additionally, by inhibiting the DNA-PKcs signaling pathway, bevacizumab was found to improve the radiotherapy sensitivity of non-small cell lung cancer cells [26]. Anti-VEGF therapy has been shown to promote radiation-induced apoptosis in glioblastoma cells by inhibiting ataxia telangiectasia mutated (ATM) and DNA-PKcs activity [27]. In the present study, we discovered no significant difference in γH2AX expression between the Endostar combination group and the RT monotherapy group at 1 hour after treatment. While γH2AX expression in HUVECs remained significantly higher than that in the control group after 6 hours of treatment, it was significantly lower in the Endostar+RT group than in the RT monotherapy group, indicating that Endostar can inhibit RT-induced DNA damage repair in HUVECs *in vitro*. This hypothesis was also supported by our western blot analysis of γH2AX expression in endothelial cells. Additionally, phosphorylation of DNA-PKcs was significantly lower in the combined treatment group than in the single treatment groups and was dependent on Endostar, indicating that Endostar may inhibit DNA damage repair via the DNA-PKcs signaling pathway and induce apoptosis in HUVECs.

It was previously discovered that treatment with recombinant human endostatin prior to exposure to 8 Gy radiotherapy significantly inhibits tumor growth in an oral squamous cell carcinoma xenograft tumor model by inhibiting HIF-1 and VEGF expression in the body, thereby inducing remodeling the vascular system and improving hypoxia within the tumor [28]. Wen *et al*. [29] discovered that recombinant human endostatin combined with radiotherapy can improve the radiosensitivity of human nasopharyngeal carcinoma and lung adenocarcinoma transplanted tumors by increasing tumor cell and endothelial cell apoptosis, decreasing tumor hypoxia, and regulating vascular growth factor expression. Additionally, Jiang *et al*. [30] demonstrated that combining recombinant human endostatin with radiotherapy can effectively delay tumor growth, which may be related to improved tumor hypoxia and radiotherapy-induced angiogenesis inhibition. Winkler [31] discovered that inhibiting VEGFR2 expression can result in a "normalization window", or a period during which radiotherapy has the greatest therapeutic effect. It is characterized by an increase in tumor oxygenation, which is thought to be the basis for improved tumor radioresponsiveness. Other studies have also confirmed that recombinant human endostatin can normalize tumor blood vessels in a short period of time [32,33]. In our xenograft tumor study, Endostar treatment had no effect on tumor volume based on comparison with the control group. Although compared with that in the radiotherapy treatment group, the tumor volume in the combination treatment group was slightly reduced, the difference was not statistically significant. This outcome may be explained by a failure to administer radiotherapy during the normalization window, as well as by the mode, route, and dosage of radiotherapy. Additional research is required to determine the optimal treatment. Additionally, serum VEGF-A levels were significantly lower in the combined group compared to the control group, but not in the single treatment groups, indicating that Endostar can inhibit VEGF-A expression in combination with radiotherapy.

Microvessel density is a well-regarded indicator for determining the blood vessel density in tumor tissues. CD31 is a vasculature-specific marker expressed by proliferating endothelial cells in the vasculature. Pericytes support endothelial cells, and αSMA expression is a marker of pericyte coverage and vascular maturity. In a colorectal cancer xenograft model, the microvessel density in the tumor tissue of the radiotherapy treatment group was significantly increased compared with that in the control group, whereas recombinant human endostatin combined with the radiotherapy treatment induced a significant decrease in the microvessel density within tumor tissue [34]. The findings of the present study revealed that, the expression of CD31 in the tumor tissues of the Endostar combined radiotherapy treatment group was lower than that in the radiation monotherapy group, but the expression of αSMA did not change significantly, indicating that Endostar can further inhibit radiotherapy-induced microangiogenesis without having a significant impact on the pericyte coverage.

This study has several imitations. First, this study used a single high-dose irradiation because it has a greater biological effect than segmented irradiation and can shorten the research period for smaller tumors. However, in clinical practice radiotherapy is divided into multiple doses. Second, there were only five mice in each group, making it difficult to determine statistical significance. Third, this study did not investigate hypoxia within tumor tissues or DNA damage repair in endothelial cells *in vivo*. Furthermore, orthotopic models and survival studies will be more useful for predicting the effectiveness of applying Endostar in clinical treatment than the method used in the present study. We will increase the sample size and improve the related *in vivo* experiments in future studies.

5. Conclusions

Endostar can synergize with irradiation to inhibit DNA damage repair and cell proliferation of endothelial cells through the VEGF pathway, thereby reducing the microvessel density in tumor tissues. Our findings provide experimental evidence and a theoretical basis for the application of Endostar in anti-cervical cancer treatment in the future.

Data Availability Statement

The datasets generated and analyzed during the current study are available from the corresponding author on reasonable request.

Author Contributions

ZX, XZ, YL and QZ conceived and designed research; ZX, XZ, HS, WL, YD, LX and HZ collected data and conducted research; ZX, YL and XZ analyzed and interpreted data; ZX and YL wrote the initial paper; YL and QZ revised the paper; YL had primary responsibility for final content. All authors read and approved the final manuscript.

Ethics Approval and Consent to Participate

The Animal Care and Use Committee approved all experimental procedures for making every effort to minimize animal suffering. All procedures were performed following the relevant guidelines and regulations.

Acknowledgment

Not applicable.

Funding

This study was funded by the China International Medical Foundation (CIMFz-2016-06-19413) and the Major Program of the Anhui Natural Science Foundation (KJ2016A754).

Conflict of Interest

The authors declare no conflict of interest.

References

[1] Bray F, Ferlay J, Soerjomataram I, Siegel RL, Torre LA, Jemal A. Global cancer statistics 2018: GLOBOCAN estimates of incidence and mortality worldwide for 36 cancers in 185 countries. CA: A Cancer Journal for Clinicians. 2018; 68: 394–424.

[2] Cohen PA, Jhingran A, Oaknin A, Denny L. Cervical cancer. Lancet. 2019; 393: 169–182.

[3] Orbegoso C, Murali K, Banerjee S. The current status of immunotherapy for cervical cancer. Reports of Practical Oncology & Radiotherapy. 2018; 23: 580–588.

[4] Karamouzis MV, Moschos SJ. The use of endostatin in the treatment of solid tumors. Expert Opinion on Biological Therapy. 2009; 9: 641–648.

[5] Limaverde-Sousa G, Sternberg C, Ferreira CG. Antiangiogenesis beyond VEGF inhibition: a journey from antiangiogenic single-target to broad-spectrum agents. Cancer Treatment Reviews. 2014; 40: 548–557.

[6] Meng F, Wang S, Yan Y, Wang C, Guan Z, Zhang J. Recombined humanized endostatin-induced suppression of HMGB1 expression inhibits proliferation of NSCLC cancer cells. Thoracic Cancer. 2019; 10: 90–95.

[7] Xu X, Mao W, Chen Q, Zhuang Q, Wang L, Dai J, *et al.* Endostar, a modified recombinant human endostatin, suppresses angiogenesis through inhibition of Wnt/β-catenin signaling pathway. PLoS ONE. 2014; 9: e107463.

[8] Ling Y, Yang Y, Lu N, You Q, Wang S, Gao Y, *et al*. Endostar, a novel recombinant human endostatin, exerts antiangiogenic effect via blocking VEGF-induced tyrosine phosphorylation of KDR/Flk-1 of endothelial cells. Biochemical and Biophysical Research Communications. 2007; 361: 79–84.

[9] Ke Q, Zhou S, Huang M, Lei Y, Du W, Yang J. Early Efficacy of Endostar Combined with Chemoradiotherapy for Advanced Cervical Cancers. Asian Pacific Journal of Cancer Prevention. 2012; 13: 923–926.

[10] Jia Y, Liu M, Huang W, Wang Z, He Y, Wu J, *et al*. Recombinant Human Endostatin Endostar Inhibits Tumor Growth and Metastasis in a Mouse Xenograft Model of Colon Cancer. Pathology & Oncology Research. 2012; 18: 315–323.

[11] Zhang K, Wang H, Wang Z, LI F, Cui Y, Ma S, *et al*. Intensity-modulated radiation therapy (IMRT)-based concurrent chemoradiotherapy (CCRT) with Endostar in patients with pelvic locoregional recurrence of cervical cancer. Medicine. 2020; 99: e21966.

[12] Viallard C, Larrivée B. Tumor angiogenesis and vascular normalization: alternative therapeutic targets. Angiogenesis. 2017; 20: 409–426.

[13] Pueyo G, Mesia R, Figueras A, Lozano A, Baro M, Vazquez S, *et al*. Cetuximab may Inhibit Tumor Growth and Angiogenesis Induced by Ionizing Radiation: a Preclinical Rationale for Maintenance Treatment after Radiotherapy. The Oncologist. 2010; 15: 976–986.

[14] Xu Z, Shu H, Zhang F, Luo W, Li Y, Chu J, *et al.* Nimotuzumab Combined With Irradiation Enhances the Inhibition to the HPV16 E6-Promoted Growth of Cervical Squamous Cell Carcinoma. Frontiers in Oncology. 2020; 10: 1327.

[15] Sedelnikova OA, Horikawa I, Redon C, Nakamura A, Zimonjic DB, Popescu NC, *et al*. Delayed kinetics of DNA double-strand break processing in normal and pathological aging. Aging Cell. 2008; 7: 89–100.

[16] FOLKMAN J. Antiangiogenesis in cancer therapy—endostatin and its mechanisms of action. Experimental Cell Research. 2006; 312: 594–607.

[17] Luo H, Xu M, Zhu X, Zhao J, Man S, Zhang H. Lung cancer cellular apoptosis induced by recombinant human endostatin gold nanoshell-mediated near-infrared thermal therapy. International Journal of Clinical and Experimental Medicine. 2015; 8: 8758–8766.

[18] Zhang L, Ge W, Hu K, Zhang Y, Li C, Xu X, *et al*. Endostar down-regulates HIF-1 and VEGF expression and enhances the radioresponse to human lung adenocarcinoma cancer cells. Molecular Biology Reports. 2012; 39: 89–95.

[19] Jiang X, Qiao Y, Dai P, Chen Q, Wu J, Song D, *et al*. Enhancement of Recombinant Human Endostatin on the Radiosensitivity of Human Pulmonary Adenocarcinoma a549 Cells and its Mechanism. Journal of Biomedicine and Biotechnology. 2012; 2012: 301931.

[20] Fukumoto S, Morifuji M, Katakura Y, Ohishi M, Nakamura S. Endostatin inhibits lymph node metastasis by a down-regulation of the vascular endothelial growth factor C expression in tumor cells. Clinical & Experimental Metastasis. 2005; 22: 31–38.

[21] Di Micco R, Fumagalli M, Cicalese A, Piccinin S, Gasparini P, Luise C, *et al*. Oncogene-induced senescence is a DNA damage response triggered by DNA hyper-replication. Nature. 2006; 444: 638–642.

[22] Toulany M, Kehlbach R, Florczak U, Sak A, Wang S, Chen J, *et al*. Targeting of AKT1 enhances radiation toxicity of human tumor cells by inhibiting DNA-PKcs-dependent DNA double-strand break repair. Molecular Cancer Therapeutics. 2008; 7: 1772–1781.

[23] Friedmann BJ, Caplin M, Savic B, Shah T, Lord CJ, Ashworth A, *et al*. Interaction of the epidermal growth factor receptor and the DNA-dependent protein kinase pathway following gefitinib treatment. Molecular Cancer Therapeutics. 2006; 5: 209–218.

[24] Dittmann K, Mayer C, Kehlbach R, Rodemann HP. Radiation-induced caveolin-1 associated EGFR internalization is linked with nuclear EGFR transport and activation of DNA-PK. Molecular Cancer. 2008; 7: 69.

[25] Yan H, Guo W, Li K, Tang M, Zhao X, Lei Y, *et al*. Combination of DESI2 and endostatin gene therapy significantly improves antitumor efficacy by accumulating DNA lesions, inducing apop-

tosis and inhibiting angiogenesis. Experimental Cell Research. 2018; 371: 50–62.
[26] Gao H, Xue J, Zhou L, Lan J, He J, Na F, *et al*. Bevacizumab radiosensitizes non-small cell lung cancer xenografts by inhibiting DNA double-strand break repair in endothelial cells. Cancer Letters. 2015; 365: 79–88.
[27] Brown CK, Khodarev NN, Yu J, Moo-Young T, Labay E, Darga TE, *et al*. Glioblastoma cells block radiation-induced programmed cell death of endothelial cells. FEBS Letters. 2004; 565: 167–170.
[28] Zhu H, Yang X, Ding Y, Liu J, Lu J, Zhan L, *et al*. Recombinant human endostatin enhances the radioresponse in esophageal squamous cell carcinoma by normalizing tumor vasculature and reducing hypoxia. Scientific Reports. 2015; 5: 14503.
[29] Wen Q, Meng M, Yang B, Tu L, Jia L, Zhou L, *et al*. Endostar, a recombined humanized endostatin, enhances the radioresponse for human nasopharyngeal carcinoma and human lung adenocarcinoma xenografts in mice. Cancer Science. 2009; 100: 1510–1519.
[30] Jiang X, Dai P, Wu J, Song D, Yu J. Inhibitory effect of radiotherapy combined with weekly recombinant human endostatin on the human pulmonary adenocarcinoma a549 xenografts in nude mice. Lung Cancer. 2011; 72: 165–171.
[31] Winkler F, Kozin S, Tong R, Chae S, Booth M, Garkavtsev I, *et al*. Kinetics of vascular normalization by VEGFR2 blockade governs brain tumor response to radiationRole of oxygenation, angiopoietin-1, and matrix metalloproteinases. Cancer Cell. 2004; 6: 553–563.
[32] Fukumura D, Jain RK. Tumor microvasculature and microenvironment: Targets for anti-angiogenesis and normalization. Microvascular Research. 2007; 74: 72–84.
[33] Huang G, Chen L. Recombinant human endostatin improves anti-tumor efficacy of paclitaxel by normalizing tumor vasculature in Lewis lung carcinoma. Journal of Cancer Research and Clinical Oncology. 2010; 136: 1201–1211.
[34] Zhang K, Wang Y, Yu X, Shi Y, Yao Y, Wei X, *et al.* Recombinant human endostatin combined with radiotherapy inhibits colorectal cancer growth. BMC Cancer. 2017; 17: 899.